nature portfolio

Peer Review File

Joint Subarray Acoustic Tweezers Enable Controllable Cell Translation, Rotation, and Deformation

REVIEWER COMMENTS

Reviewer #1 (Remarks to the Author):

This paper represents a tour de force in microscale acoustic tweezing. The device described is by some considerable margin the most sophisticated acoustic tweezer yet developed. As such, the paper describes a significant step forward and so is certainly at the level needed for publication in Nature Communications. It is also very clearly written with great schematics! The 6 degrees of freedom (DOF) is achieved with a novel surface acoustic wave (SAW) array. This cleverly makes use of the fact that SAW devices can be mounted such the waves can pass through another SAW. Hence the array can be packing into a confined space. This novel, and actually quite simple, array design is the key to unlocking the 6DOF described here. This capability is then achieved using a combination of radiation forces for the 3 translations and streaming for the 3 rotations. Whilst various aspects of this design have been published before by the authors, combining them all in a single device here is a first – and a significant one. The paper then demonstrates that control is achieved across all these DOFs on living cells. This is impressive as cells are much harder to handle than the calibration beads often explored in such devices. Furthermore, they also show that the streaming forces are sufficient to cause cell deformation. This is a very exciting prospect as it potentially opens a capability similar to the optical tweezer-based deformation devices which have seen significant interest. As well as the experimental demonstration, which is the main result, the DOF mechanisms are simulated so that the reader can have some confidence that the described mechanisms are indeed the correct ones. Whilst these aspects are not surprising, they are useful and give further confidence in the robustness of the device concept.

Below are some issues that the authors should consider prior to publication.

1) The reader could get the impression (e.g. from fig 1a) that the device is somehow focused and that the manipulations are all performed at the focal point. However, my understanding is that within the devices are many trapping regions and that the describe operations would happen similarly to particles in any of these locations. 1) Can the authors include a diagram/schematic (probably in the SI) that conveys this multi-potential well reality. 2) Can the authors comment on the extent to which the behaviours of particles in the various (and I suppose there are thousands) potential wells are similar?

2) When the SAW device is first described, it would be worthwhile to contrast this design with what might be possible with a bulk wave design. Certainly, in a bulk wave design it would not be possible to mount one set of elements in the direct path of another. This attribute of SAWs therefore opens up the design space considerably.
3) In the introduction it would be good to comment (and briefly compare) the current devices to lower-frequency in-air manipulation devices. Some of these have also achieved 6DOF manipulation, albeit at a much larger scale (e.g. [1]). In this case only non-spherical objects could be rotated, and this was achieved using radiation forces. However, other in-air devices have used streaming for rotation (see early example in [2]).
4) Can the authors comment on the viability of the cells post manipulation? In particular viability after the streaming-induced deformation.
[1] Marzo, A., & Drinkwater, B. W. (2019). Holographic acoustic tweezers. Proceedings of the National Academy of Sciences, 116(1), 84–89.
[2] Busse, F. H., & Wang, T. G. (1981). Torque generated by orthoganal acoustic waves - theory. Journal of the Acoustical Society of America, 69(6), 1634–1638.

Reviewer #2 (Remarks to the Author):

In this paper, the authors introduce a new device that combines three levels of IDTs to control the rotation and translation of cells. Overall, the paper is original and introduces some new possibilities for SAW-based tweezers, which open perspectives in 3D imaging, disease diagnostics and drug testing, as underlined by the authors. The application to tissue engineering is more questionable since no manipulation of multiple objects is demonstrated.

The control of the position and orientation of cells is highly challenging, and the authors have performed a nice piece of work, which definitely deserves publication. Nevertheless, the following points should be carefully addressed for consideration in a high impact journal such as Nature Communications.

First, the authors should clarify not only the possibilities but also the limits of their device:

(i) The first and most important point is that “degrees of freedoms” are by definition independent. In the present cases, the control of the translation and rotation are definitely not independent, contrary to the claims of the paper. The following dependencies are clear from the data of the paper:

• In the (x,y) plane translation and rotation can only be controlled independently along the same axis. The translation along y movement and rotation along x are (a) not convincing since the video shows a translation that is not straight and over less than a cell diameter (movie S8), (b) not independent since they rely on a combined effect of streaming and radiation pressure (produced by the same IDTs) that cannot be separately activated.

• According to the invoked mechanisms, all the rotations along x,y and z axes, will produce a drag force along the z-axis, which will destabilize the fragile levitation equilibrium of the cell. Rotations are hence expected to influence the z-position of the cell.

So, the word independent should be removed from the manuscript, and the dependencies among the degrees of freedom be clarified in the title, abstract and conclusion of the paper.

(ii) Instead of claiming independent DoFs, the authors could claim sequential control of rotation and translation of cells (which is already a strong achievement). But additional data should be provided to support this claim. Indeed it is not clear to which extent the different rotation can be controlled whatever the position of the cell in the (x,y,z) space. So, it is essential to provide a single experiment with successive displacements along x, y and z interspersed with the 3 rotations, to demonstrate that sequential control of the different degree of freedom is possible.

(iii) Following the previous points, the authors must clarify the acoustic scene wherein each degree of freedom can be effectively controlled, i.e. in which region the particle can be displaced and in which region each rotation can be precisely controlled. This point must be supported by experimental data.

(iv) The authors must clearly indicate in the manuscript that contrary to the (x,y) directions, there is not acoustic trap in the z-direction but only levitation resulting from a fragile equilibrium between different forces. Indeed, a trap indicates a restoring force that tends to

bring back a particle to the equilibrium position when perturbated. There is no such restoring force in the present case. It means that if gravity was inverted or in presence of fluctuating external flow, no equilibrium could be reached. In particular streaming and radiation force cannot compensate one-another since they are both proportional to the beam intensity. In addition, no control of the z position is demonstrated in the present paper since the cell seems only to be pushed from the bottom of the chamber to the top of the chamber. It is not clear that the particle could be stabilized at intermediate position, especially if other degree of freedoms (especially rotation) would be activated. All these points should be clarified.

The second essential point is that no data is provided on cells viability and on temperature variations induced by the acoustical tweezers. Study of cells viability in conditions of power and duration of activation similar to the ones used to perform the translation and rotation of cells are mandatory to assess the potential of these tweezers for biological applications. Temperature increase should also be monitored for the different operations (translation, rotation) since, compared to their previous publications, the authors use higher frequency tweezers (for the rotation control) that are expected to produce larger dissipation and hence temperature increase. By the way, the actuation frequencies of the different IDTs are not specified. They should be specified in the main part of the manuscript.

From a physical point of view,

(i) The model used to simulate acoustic streaming only accounts for Eckart bulk streaming, not boundary Rayleigh streaming. This should be both specified and justified in the manuscript. Indeed, according to the work by Bruus [Bruus H. 3D modeling of acoustofluidics in a liquid-filled cavity including streaming, viscous boundary layers, surrounding solids, and a piezoelectric transducer. Mathematics, (2019)], we could expect both bulk and boundary streaming to be significant in this type of configurations.
(ii) I do not understand why for the control of the z position (Fig 2d), the direction of the radiation force and streaming force are opposite to what was calculated in Ref. 2 (Fig. 4), while the devices look pretty similar. Could you please clarify this point?

In addition, time scales must be specified in all the figures and additional videos.

Reviewer #3 (Remarks to the Author):

Novelty:

This paper demonstrates the feasibility of combining in the same device, several operations related to translation, rotation, and deformation of a single cell by surface acoustic waves. A major novelty lies in that operations of translation, rotation, and deformation, which have been demonstrated separately before, are here combined in the same chip. It is impressive.

Major things:

I realize that the authors have a challenge in explaining all the features of the device since it has so many degrees of freedom, and a journal paper is just in 2D. By just reading the manuscript it is difficult to understand if the method is robust and predictable. The videos helps. Nevertheless, I have some questions and comments. Overarching, it is difficult to understand to what extent the translations are predictable and if any calibrations are done.

What parameters are controlled in the Matlab code? Which of these are kept constant during the operation and which are being adjusted? Please describe the main features of the program.

Please describe how the motion of a cell is programmed, like when you make the letters ‘D’, ‘U’, ‘K’, ‘E’. Can you program an arbitrary trajectory based on a rule or a function, or it must be tweaked? Do you need to calibrate the phase shift necessary to achieve a certain translation? It would be very convincing if you could overlay the intended trajectory with the measured trajectory.

Looking at movies S3 and S4, I do not understand how a symmetric streaming field can lead to rotation of the cell if it is positioned in the center of the channel. I would expect the net rotation to be zero. I understand that when a cell is held in position by one acoustic field while the fluid is streaming vigorously, it is likely that it will gain some net rotation, but how can it be predicted? Again, is it programmed from first principles, or does one need to find

suitable combinations of sound fields by scanning through frequencies, amplitudes, and phase shifts?

If I understand it correctly, the rotation around x- and y is governed by the 'mid' transducers. How can a cell rotate consistently while moving across a streaming field that is not constant? Or do you need to adjust the 'mid' transducer for each position? Describe how this is done.

The z-translation has quite limited data. What is the range that you can translate the cell? How fast does it respond to a change in amplitude? I.e. does it rely on sedimentation to go down or the streaming takes care of it?

Cell deformation has previously been demonstrated experimentally and theorized upon in the realm of bulk-acoustic waves, some works of which should be cited IMHO (DOI: 10.1103/physreve.99.063002, DOI: 10.1063/5.0122017, DOI: 10.1039/c9lc00999j, DOI: 10.1063/1.4882777).

Minor things:
The start of movie S3 is a bit chaotic and it is not easy to observe the streaming field at the beginning.

Fig 2D, streaming arrows are too small.

Figure S1 and S2: Show scale bar.

Per Augustsson
Lund University
Sweden

Itemized list of response to reviewers' remarks

(*Black italic: Editor's remarks*; Blue type: Our response; Additions/modifications to the manuscript and Supplementary Materials are highlighted in yellow)

Reviewer: #1

Comment: *This paper represents a tour de force in microscale acoustic tweezing. The device described is by some considerable margin the most sophisticated acoustic tweezer yet developed. As such, the paper describes a significant step forward and so is certainly at the level needed for publication in Nature Communications. It is also very clearly written with great schematics! The 6 degrees of freedom (DOF) is achieved with a novel surface acoustic wave (SAW) array. This cleverly makes use of the fact that SAW devices can be mounted such the waves can pass through another SAW. Hence the array can be packing into a confined space. This novel, and actually quite simple, array design is the key to unlocking the 6DOF described here. This capability is then achieved using a combination of radiation forces for the 3 translations and streaming for the 3 rotations. Whilst various aspects of this design have been published before by the authors, combining them all in a single device here is a first – and a significant one. The paper then demonstrates that control is achieved across all these DOFs on living cells. This is impressive as cells are much harder to handle than the calibration beads often explored in such devices. Furthermore, they also show that the streaming forces are sufficient to cause cell deformation. This is a very exciting prospect as it potentially opens a capability similar to the optical tweezer-based deformation devices which have seen significant interest. As well as the experimental demonstration, which is the main result, the DOF mechanisms are simulated so that the reader can have some confidence that the described mechanisms are indeed the correct ones. Whilst these aspects are not surprising, they are useful and give further confidence in the robustness of the device concept. Below are some issues that the authors should consider prior to publication.*

Our response: We thank the reviewer for the positive comments on this work and for giving several important comments that are very helpful to further improve the manuscript. All of your comments have been addressed. Point-by-point responses to your comments are given below.

Comment 1: *The reader could get the impression (e.g. from fig 1a) that the device is somehow focused and that the manipulations are all performed at the focal point. However, my understanding is that within the devices are many trapping regions and that the describe operations would happen similarly to particles in any of these locations. 1) Can the authors include a diagram/schematic (probably in the SI) that conveys this multi-potential well reality. 2) Can the authors comment on the extent to which*

the behaviours of particles in the various (and I suppose there are thousands) potential wells are similar?

Our response: We thank the reviewer for this comment. Per the reviewer's comment, we have revised Supplementary Figure 1 to show multiple potential wells and each of them can trap a particle for manipulation.

The ability to manipulate multiple particles depends on the SAW wavelength and the microfluidic chamber's size. For example, when the wavelength of SAWs generated by all the outer IDTs (*i.e.*, $\{IDT_i^{out}\}_4$) is 200 μm and the chamber dimension is 425 μm × 425 μm (425 μm is slightly larger than two wavelengths), the number of generated potential wells is 5 × 5 = 25. Hence, these 25 potential wells can trap particles to perform manipulation.

Changes to the manuscript: Per the reviewer's comment, we made the following changes.

- In the "Mechanisms of JSAT" section of the manuscript, we have added the following text: "one of multiple Gor'kov potential wells"
- Updated Supplementary Figure 1

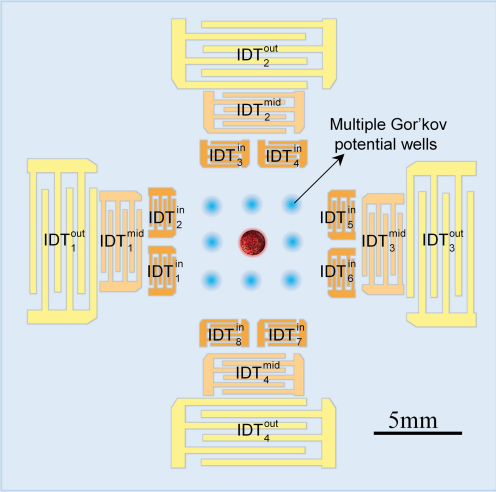

- In the caption of Supplementary Figure 1, we added the following text: "Multiple Gor'kov potential wells (*i.e.*, 3×3 potential wells illustrated by blue spots) can be generated in a microfluidic chamber at the array center when all the outer IDTs are excited to trap cells. For example, a cell (illustrated by a red sphere) is trapped at the center well of a 3×3 well array."

Comment 2: *When the SAW device is first described, it would be worthwhile to contrast this design with what might be possible with a bulk wave design. Certainly, in a bulk wave design it would not be possible to mount one set of elements in the direct path of another. This attribute of SAWs therefore opens up the design space considerably.*

Our response: We thank the reviewer for this comment. The propagation of bulk acoustic waves generated by a PZT can be impeded when another PZT is situated in the wave propagation path, thus hindering the parallel integration of multiple PZTs for complex functionalities. Conversely, surface acoustic waves generated by an interdigital transducer (IDT) exhibit good transmissibility through regions with other IDTs, thereby allowing more options for designing complex IDT arrays.

Changes to the manuscript: Per the reviewer's comment, in Section "Mechanisms of JSAT", we added the following text: "Such design is difficult to achieve using thickness-mode piezoelectric transducers (such as PZTs), as the bulk acoustic waves generated by a PZT are impeded by other PZTs placed in the wave propagation path. This limits the options of integrating multiple PZTs for achieving complex cell/particle manipulation functions. Conversely, SAWs generated by an IDT exhibit good transmissibility through regions with IDTs working at different frequencies, thereby allowing more options for designing complex IDT arrays."

Comment 3: *In the introduction it would be good to comment (and briefly compare) the current devices to lower-frequency in-air manipulation devices. Some of these have also achieved 6DOF manipulation, albeit at a much larger scale (e.g. [1]). In this case only non-spherical objects could be rotated, and this was achieved using radiation forces. However, other in-air devices have used streaming for rotation (see early example in [2]).*

[1] Marzo, A., & Drinkwater, B. W. (2019). Holographic acoustic tweezers. Proceedings of the National Academy of Sciences, 116(1), 84–89.

[2] Busse, F. H., & Wang, T. G. (1981). Torque generated by orthoganal acoustic waves - theory. Journal of the Acoustical Society of America, 69(6), 1634–1638.

Our response: We thank the reviewer for this comment. In paper [1], Marzo and Drinkwater developed holographic acoustic tweezers, which used an array of low-frequency transducers to generate and control airborne acoustic waves for positioning and orienting multiple objects in the air. In paper [2], Busse and Wang presented a theoretical framework for predicting the torque induced by orthogonal acoustic waves for rotational manipulation.

Changes to the manuscript: Per the reviewer's comments, the revised manuscript cited the two important papers suggested by the reviewer. In addition, in the "Introduction", we have added the following text: " For rotational object manipulation, an early study by Busse and Wang presented a theoretical framework to predict the torque indued by orthogonal acoustic waves[63]. To achieve both

translational and rotational manipulation of acoustically trapped objects, Marzo and Drinkwater developed holographic acoustic tweezers, leveraging an array of transducers to generate airborne acoustic waves and reshape the acoustic energy field to versatile patterns[64]. However, as this method uses airborne acoustic waves, it is limited to manipulating objects in the air[64]. ”

Comment 4: *Can the authors comment on the viability of the cells post manipulation? In particular viability after the streaming-induced deformation.*

Our response: Thanks for the comment. We performed a cell viability test with N=152 cells. MCF7 cells were first stained with calcein-AM (C3100MP, Life Technologies) for showing live cells (green fluorescence) and propidium iodide (FP028, ABP Biosciences) for showing dead cells (red fluorescence). The cells were then injected into a microchamber and subjected to acoustic waves generated by a pair of IDTs in the middle subarray, connected to electrical signals with a voltage of 10 Vpp for 120 seconds. The whole acoustic exposure process is recorded in the supplementary movie S11. Recorded fluorescence images for a test group are given in Fig. R4.1 (a-d). We repeated the viability test procedure multiple times (N=21), as the used cell chamber only held a small number of cells. Fig. R4.1(e) summarizes the experimentally obtained cell viability data for N=152 cells, indicating a high cell viability of 99.3% after 120 seconds of acoustic exposure.

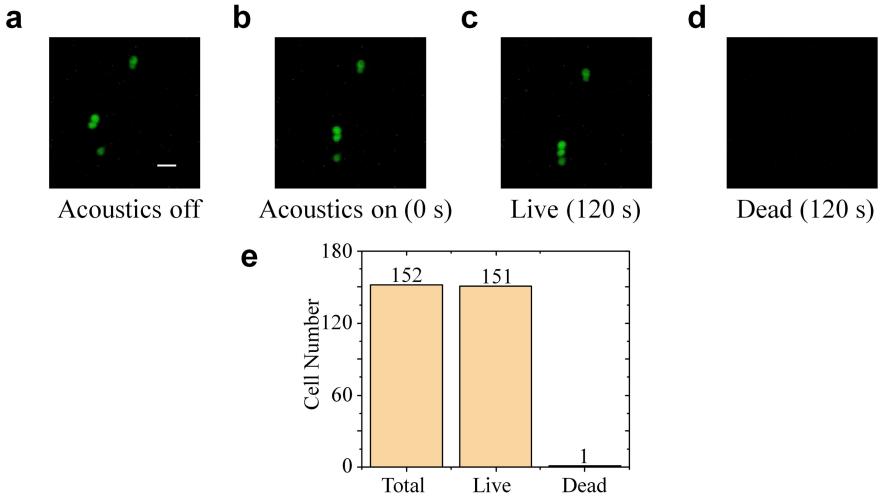

Fig. R4.1 **(a-c)** Images of the green fluorescence channel for three scenarios: **(a)** no acoustic waves applied, **(b)** acoustic waves turned on, **(c)** 120 seconds of acoustic exposure. In these images, the green dots are cells stained with calcium-AM. **(d)** Image of the red fluorescence channel acquired after 120 seconds of acoustic exposure (Scale bar: 40 μm). This image is black indicating no dead cells in that test group, due to the lack of uptake of propidium iodide. **(e)** Summarized cell viability data for all the N=152 cells across multiple tests (N=21).

Changes to the manuscript: Per the reviewer's comments, we made the following changes.

- In the "Cell deformation measurement" subsection of "Materials and Methods", we added the text: "In addition, we measured the SAW device's temperature, as well as the post-treatment cell viability. Their detailed procedures and results are in Supplementary Note 3 and Supplementary Figures 13-15".
- In the Supplementary Information, we have added detailed test procedures.

In addition, we performed a cell viability test with N=152 cells. MCF7 cells were first stained with calcein-AM (C3100MP, Life Technologies) for showing live cells (green fluorescence) and propidium iodide (FP028, ABP Biosciences) for showing dead cells (red fluorescence). The cells were then injected into a microchamber and subjected to acoustic waves generated by the middle subarray's two IDTs excited by an input signal with a voltage of 10 Vpp for 120 seconds. The whole acoustic exposure process is recorded in the movie S11. Recorded fluorescence images for a test group are given in Supplementary Figure S15a-d. We repeated the viability test procedure multiple times (N=21), as the used cell chamber only held a small number of cells. Supplementary Figure S15e summarizes the experimentally obtained cell viability data for N=152 cells, indicating a high cell viability of 99.3% after 120 seconds of acoustic exposure.

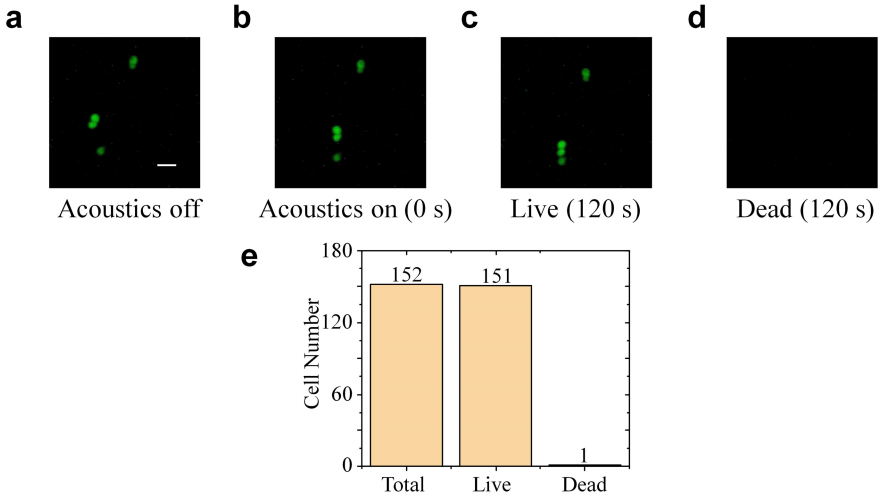

Supplementary Figure 15. Cell viability test results. (a-c) Images of the green fluorescence channel for three scenarios: **(a)** no acoustic waves applied, **(b)** acoustic waves turned on, **(c)** 120 seconds of acoustic exposure. In these images, the green dots are cells stained with calcium-AM. **(d)** Image of the red fluorescence channel acquired after 120 seconds of acoustic exposure (Scale bar: 40 μm). This image is black indicating no dead cells in that test group, due to the lack of uptake of propidium iodide. **(e)** Summarized cell viability data for all the N=152 cells in multiple tests (N=21).

Reviewer: #2

Comment: *In this paper, the authors introduce a new device that combines three levels of IDTs to control the rotation and translation of cells. Overall, the paper is original and introduces some new possibilities for SAW-based tweezers, which open perspectives in 3D imaging, disease diagnostics and drug testing, as underlined by the authors. The application to tissue engineering is more questionable since no manipulation of multiple objects is demonstrated.*

The control of the position and orientation of cells is highly challenging, and the authors have performed a nice piece of work, which definitely deserves publication. Nevertheless, the following points should be carefully addressed for consideration in a high impact journal such as Nature Communications.

Our response: We thank the reviewer for the positive comments on this work. In this study, our purpose is to develop an acoustic device and demonstrate its multiple functions of manipulating single cells. Tissue engineering is not the focus of this manuscript; hence, it is only mentioned as a potential future application in the manuscript. In tissue engineering, constructing high-resolution tissue models is a desired function. We anticipate that our tweezers can be used for this function by translating cells to desired positions in a programmable manner, and we plan to conduct this work in the future. Point-by-point responses to your comments are given below.

Comment 1: *First, the authors should clarify not only the possibilities but also the limits of their device: (i) The first and most important point is that "degrees of freedoms" are by definition independent. In the present cases, the control of the translation and rotation are definitely not independent, contrary to the claims of the paper. The following dependencies are clear from the data of the paper:*

• In the (x,y) plane translation and rotation can only be controlled independently along the same axis. The translation along y movement and rotation along x are (a) not convincing since the video shows a translation that is not straight and over less than a cell diameter (movie S8), (b) not independent since they rely on a combined effect of streaming and radiation pressure (produced by the same IDTs) that cannot be separately activated.

• According to the invoked mechanisms, all the rotations along x,y and z axes, will produce a drag force along the z-axis, which will destabilize the fragile levitation equilibrium of the cell. Rotations are hence expected to influence the z-position of the cell.

So, the word independent should be removed from the manuscript, and the dependencies among the degrees of freedom be clarified in the title, abstract and conclusion of the paper.

(ii) Instead of claiming independent DoFs, the authors could claim sequential control of rotation and translation of cells (which is already a strong achievement). But additional data should be provided to support this claim. Indeed it is not clear to which extent the different rotation can be controlled whatever the position of the cell in the (x,y,z) space. So, it is essential to provide a single experiment with successive displacements along x, y and z interspersed with the 3 rotations, to demonstrate that sequential control of the different degree of freedom is possible.

(iii) Following the previous points, the authors must clarify the acoustic scene wherein each degree of freedom can be effectively controlled, i.e. in which region the particle can be displaced and in which region each rotation can be precisely controlled. This point must be supported by experimental data.

(iv) The authors must clearly indicate in the manuscript that contrary to the (x,y) directions, there is not acoustic trap in the z-direction but only levitation resulting from a fragile equilibrium between different forces. Indeed, a trap indicates a restoring force that tends to bring back a particle to the equilibrium position when perturbated. There is no such restoring force in the present case. It means that if gravity was inverted or in presence of fluctuating external flow, no equilibrium could be reached. In particular streaming and radiation force cannot compensate one-another since they are both proportional to the beam intensity. In addition, no control of the z position is demonstrated in the present paper since the cell seems only to be pushed from the bottom of the chamber to the top of the chamber. It is not clear that the particle could be stabilized at intermediate position, especially if other degree of freedoms (especially rotation) would be activated. All these points should be clarified.

Our response: We would like to express our gratitude to the reviewer for providing these important comments. Our responses to your comments (i) to (iv) are given below.

Response to Comment (i): We agree with the reviewer's comment that the six degrees of freedom are not fully independent. Therefore, we have revised the manuscript by changing the term 'Six Degrees-of-Freedom Acoustic Tweezers' to 'Joint Subarray Acoustic Tweezers'.

- We want to clarify that our acoustic tweezers can achieve the following complex controls

Independent control of 3D translation u_x, u_y, and u_z	Control of u_x: Change input phase difference for IDT_1^{out} and IDT_3^{out} Control of u_y: Change input phase difference for IDT_2^{out} and IDT_4^{out} Control of u_z: Change input time for IDT_1^{out} to IDT_4^{out}
Independent control of 3D rotation θ_x, θ_y, and θ_z	Control of θ_x: Change amplitudes to control streaming generated by IDT_2^{mid} and IDT_4^{mid} Control of θ_y: Change amplitudes to control streaming generated by IDT_1^{mid} and IDT_3^{mid} Control of θ_z: Change amplitudes to control streaming generated by transducers selected from IDT_1^{in} to IDT_8^{in}

Independent control of translation u_x and rotation θ_x	Control of u_x: Change input phase difference for IDT_1^{out} and IDT_3^{out} Control of θ_x: Change amplitudes to control streaming generated by IDT_2^{mid} and IDT_4^{mid}
Independent control of translation u_x and rotation θ_y	Control of u_x: Change phase difference for IDT_1^{mid} and IDT_3^{mid} To avoid non-straight translation: Use standing waves generated by IDT_2^{out} and IDT_4^{out} Control of θ_y: Change amplitude difference for IDT_1^{mid} and IDT_3^{mid}
Independent control of translation u_x and rotation θ_z	Control of u_x: Change input phase difference for IDT_1^{out} and IDT_3^{out} To avoid non-straight translation: Use standing waves generated by IDT_2^{out} and IDT_4^{out} Control of θ_z: Change amplitudes to control streaming generated by transducers selected from IDT_1^{in} to IDT_8^{in}
Independent control of translation u_y and rotation θ_x	Control of u_y: Change phase difference for IDT_2^{mid} and IDT_4^{mid} to control translation To avoid non-straight translation: Use standing waves generated by IDT_1^{out} and IDT_3^{out} Control of θ_x: Change amplitude difference for IDT_2^{mid} and IDT_4^{mid}
Independent control of translation u_y and rotation θ_y	Control of u_y: Change input phase difference for IDT_2^{out} and IDT_4^{out} Control of θ_y: Change amplitude difference for IDT_1^{mid} and IDT_3^{mid}
Independent control of translation u_y and rotation θ_z	Control of u_y: Change input phase difference for IDT_2^{out} and IDT_4^{out} To avoid non-straight translation: Use standing waves generated by IDT_1^{out} and IDT_3^{out} Control of θ_z: Change amplitudes to control streaming generated by transducers selected from IDT_1^{in} to IDT_8^{in}

As summarized in the table, our device can achieve various combined rotational and translational motions. These different combinations verified in our experiments have not been achieved by the array of microscale acoustic tweezers. Per the reviewer's comment, we have updated movie S8 to show a longer range. When performing combined translation and rotation, the non-straight translation can be corrected by turning on the outer layer IDTs. For example, if we want to achieve straight translation u_y and rotation θ_x, we can turn on IDT_1^{out} and IDT_3^{out} to stabilize the object in the *x*-direction.

Our approach can achieve independent control of translation and rotation, even when the translation axis and the rotation axis are orthogonal. For example, to independently control translation u_x along the x-axis and rotation θ_y with respect to the y-axis, we can change the phase difference for IDT_1^{mid} and IDT_3^{mid} to control translation and change the amplitude difference for IDT_1^{mid} and IDT_3^{mid} to control streaming-induced rotation. With the input phase control and amplitude control, translational and rotational motions can be independently controlled.

We agree with the reviewer that the drag force during three-dimensional rotation destabilizes the z-position due to the fragile levitation equilibrium. Therefore, we have removed the term "independent" from the manuscript and no longer claim independence in z-translation. While fully

independent 6 DoF manipulation is challenging, our tweezers achieve all basic motions (u_x, u_y, u_z, θ_x, θ_y, and θ_z) and even cell deformation.

Response to Comment (ii) and (iii): We appreciate the reviewer's suggestion. Sequential control of rotation and translation is achievable with our acoustic tweezers because (1) all six motions (u_x, u_y, u_z , θ_x, θ_y, and θ_z) are verified by the theoretical analysis and the experimental results in Fig 2 and 3, and (2) these motions can occur throughout the entire microfluidic chamber surrounded by the IDT array. For example, (a) the cell translation along a "D" trajectory in the upper left side of the chamber was demonstrated in Fig. R1.1. This means our device can conduct cell manipulation in the whole microfluidic chamber according to the principle of symmetry. The pressure nodes used for cell trapping and translation are distributed throughout the whole chamber, as found in a previous study (*Collins DJ, Morahan B, Garcia-Bustos J, Doerig C, Plebanski M, Neild A. Two-dimensional single-cell patterning with one cell per well driven by surface acoustic waves. Nat Commun 6, 8686 (2015)*). (b) The streaming vortices used for rotating in θ_x (or θ_y) direction and θ_z direction occur throughout the chamber as shown in Fig. R1.2 and Fig. S8c. Therefore, the corresponding region in which cells can be rotated and translated is the chamber size (300 μm×300 μm×60 μm).

In addition to sequential control, we think another significant contribution is achieving various combined motions with translation and rotation independently controlled, as shown in Fig. 4. Other acoustic tweezers are not able to achieve those various combinations (summarized in the table) of independently controlled rotational and translational motions.

Response to Comment (iv): We appreciate the reviewer's comment on z-directional manipulation. As shown in Fig. 2d (right), the out-of-plane motion u_z is dependent on the interplay of all the out-of-plane forces, including the position-dependent acoustic radiation and drag forces, the buoyancy force F_{Buo}, and the gravitational force F_g. Most cells, including MCF7 cells, have a density slightly higher than the culture medium (water with additives), so the z-directional manipulation can be controlled theoretically by applying a precise input power to match to account for the aforementioned out-of-plane forces. However, as pointed out by the reviewer, the out-of-plane manipulation cannot be as precise and stable as the in-plane manipulation due to the absence of a Gor'kov potential well-like trap. In addition, our z-manipulation approach also has the following limitations. The manipulation precision is hindered by our currently used microscope's two-dimensional imaging limitation, and other motions, especially rotational motions, affect z-directional translation. Per the reviewer's comment, we have discussed these limitations in the revised manuscript.

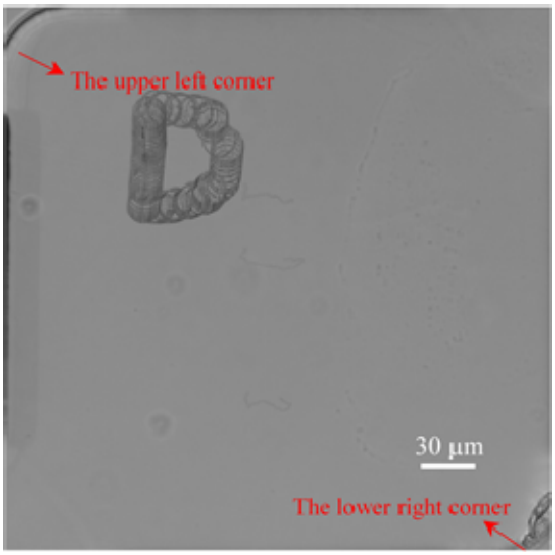

Fig. R1.1 Stacked image showing cell translation along a "D" trajectory within a microfluidic chamber. This translation is performed near the upper left corner of the chamber.

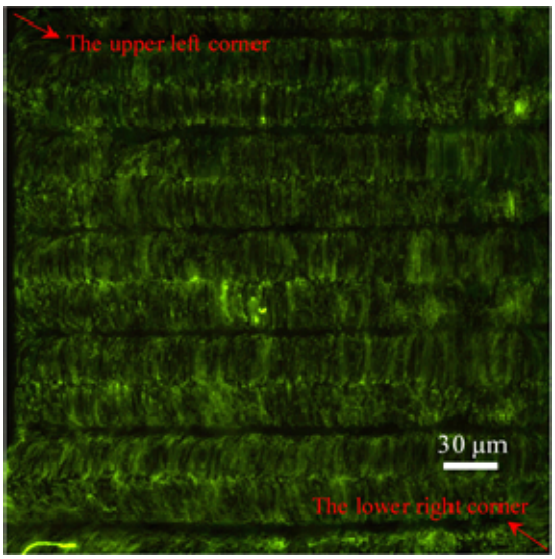

Fig. R1.2 Visualization of acoustic streaming vortices for rotating cells in the θ_x direction. The streaming pattern covers the entire microfluidic chamber.

Changes to the manuscript: Per the reviewer's comment, we made the following changes.

- Changed the title to "Joint Subarray Acoustic Tweezers Enable Controllable Cell Translation, Rotation, and Deformation"
- Updated the abbreviation from "6DAT" to "JSAT"
- Updated "six DoFs" to "six fundamental motions".
- We have deleted the claims about independently controlling the 6-DoF motions

- In the “Abstract”, we updated the text: “However, current tweezers are limited in their ability to comprehensively manipulate bioparticles, providing only partial control over the six fundamental motions (three translational and three rotational motions). This study presents a joint subarray acoustic tweezers (JSAT) platform that leverages acoustic radiation force and viscous torque to control the six fundamental motions of single bioparticles. This breakthrough is significant as our manipulation mechanism allows for controlling the three translational and three rotational motions of single cells, as well as enabling complex manipulation that combines controlled translational and rotational motions.”
- In the “Introduction” section, we have updated the text “is able to control all the six fundamental motions and achieve complex manipulation combined with controlled translational and rotational motions, thus facilitating comprehensive cell manipulation in a 3D space”; “allows for controlling the six fundamental (three translational and three rotational) motions of single cells, achieving complex motions with controlled translation and rotation, and deforming an acoustically trapped cell”; and “Moreover, few studies investigate the mechanisms to achieved complex manipulation that combines controlled translation and rotation of single cells.”
- In the “3D translation *via* JSAT”, we updated and added the text: “which points to the +*z*-direction acting as the levitation driving force” and “The out-of-plane translation u_z depends on the interplay of all the out-of-plane forces, including the position-dependent acoustic radiation and drag forces, the buoyancy force F_{Buo}, and the gravitational force F_g, as shown in Fig. 2d (right). Most cells, including MCF7 cells, have a density slightly higher than the culture medium (water with additives), so the z-directional manipulation can be controlled theoretically by applying a precise input power to match to account for the aforementioned out-of-plane forces. However, the control of out-of-plane translation cannot be as precise and stable as the control of in-plane translation due to the absence of a Gor’kov potential well-like trap. Additionally, when the cell experiences other motions, especially rotational motions, they affect the out-of-plane translation. The out-of-plane translation precision is also affected by the two-dimensional imaging nature of our current microscope, as the translation is difficult to be quantitively monitored.”
- In the “Simultaneous translation and rotation via JSAT” section, we added the text: “Although both acoustic radiation force and streaming are generated by the same IDTs, the translation u_x is controlled by the input phase difference, and the rotation θ_y is controlled by the input amplitude difference between the two IDTs. Hence, the involved translational and rotational motions could be independently controlled.”

- In the "Discussion" section, we updated the text: "With the aforementioned features, such as achieving the six fundamental motions of single cells and locally deforming a cell, our JSAT platform represents a significant advancement compared to previous technologies, such as optical, magnetic, and acoustic tweezers."
- In the caption of **Fig.2 (e)**, we updated the text to "When activating the IDTs for 1.6 s, the microscopic image of an MCF7 cell becomes out of focus due to the cell's *z*-position change."
- Updated movie S8

Comment 2: *The second essential point is that no data is provided on cells viability and on temperature variations induced by the acoustical tweezers. Study of cells viability in conditions of power and duration of activation similar to the ones used to perform the translation and rotation of cells are mandatory to assess the potential of these tweezers for biological applications. Temperature increase should also be monitored for the different operations (translation, rotation) since, compared to their previous publications, the authors use higher frequency tweezers (for the rotation control) that are expected to produce larger dissipation and hence temperature increase. By the way, the actuation frequencies of the different IDTs are not specified. They should be specified in the main part of the manuscript.*

Our response: We thank the reviewer for this comment. In the JSAT device, IDTs in the outer layer generate 200 μm-wavelength SAWs at 19.8 MHz (IDT_1^{out} and IDT_3^{out}) and 18.1 MHz (IDT_2^{out} and IDT_4^{out}) for translating a cell in the u_x-and u_y-directions. IDTs in the middle layer generate 100 μm-wavelength SAWs at 39.6 MHz (IDT_1^{mid} and IDT_3^{mid}) and 36.2 MHz (IDT_2^{mid} and IDT_4^{mid}) for rotating a cell in the θ_y- and θ_x-directions. IDTs in the inner layer generate 40 μm-wavelength SAWs at 98.9 MHz (IDT_1^{in}, IDT_2^{in}, IDT_5^{in}, and IDT_6^{in}) and 95.1 MHz (IDT_3^{in}, IDT_4^{in}, IDT_7^{in}, and IDT_8^{in}) to rotate a cell in the θ_z-direction. Previously, high-frequency traveling and standing SAWs generated by IDTs were used to separate and pattern cells in microfluidic chambers, similar to our SAW devices having high-frequency IDTs and a microfluidic chamber, and they showed good cell viability (*Collins DJ, et al. Selective particle and cell capture in a continuous flow using micro-vortex acoustic streaming. Lab Chip 17, 1769-1777 (2017); Collins DJ, Morahan B, Garcia-Bustos J, Doerig C, Plebanski M, Neild A. Two-dimensional single-cell patterning with one cell per well driven by surface acoustic waves. Nat Commun 6, 8686 (2015).*).

For low-power SAW acoustic tweezers, the temperature generation is usually from the region where a PDMS chamber is bonded on the SAW substrate, as the wave energy dissipation in the PDMS significantly contributes to the temperature increase. To minimize this effect, we carefully designed

our PDMS chamber by minimizing the bonding region using a design in Fig. R2.1. In this design, only the red region has PDMS in contact with the substrate.

We have performed temperature measurement experiments. Due to the 5 mm thick PDMS block leading to a challenge to directly measure the temperature inside a microfluidic chamber, we measured the temperature on the back side of a thin (500 μm) $LiNbO_3$ substrate with high thermal conductivity (4-6 W/(m·K)) by using a thermal camera (Micro-epsilon/TIM400, Germany). An excitation signal with a frequency of 39.6 MHz and a voltage of 10 Vpp is applied to IDT_1^{mid} and IDT_3^{mid} in the middle layer. After 120 seconds, the temperature distribution is shown in Fig. R2.2a, and the temperature variation over time is depicted in Fig. R2.3a. The temperature change nearly stables at 120 sec with a maximum increase less than 1 °C. On the other hand, we measured the substrate temperature when exciting an inner layer IDT using a signal with a frequency of 98.9 MHz and a voltage of 10 Vpp. The temperature distribution is shown in Fig. R2.2b, and the corresponding temperature change over time is presented in Fig. R2.3b. The temperature increase was less than 2 °C. Note that these temperature measurements were performed when the bottom of the substrate was not attached to the translation stage of the microscope. When performing actual cell manipulation experiments on the microscope stage, the temperature increase should be lower, due to the heat transfer from the SAW substrate to the microscope stage. Moreover, the SAW chip can be mounted on a Peltier cooling system, as demonstrated in our previous work for temperature control. (*Zhao S, et al. A disposable acoustofluidic chip for nano/microparticle separation using unidirectional acoustic transducers. Lab Chip 20, 1298-1308, 2020*).

Per the reviewer's comment, we performed a cell viability test with N=152 cells. MCF7 cells were first stained with calcein-AM (C3100MP, Life Technologies) for showing live cells (green fluorescence) and propidium iodide (FP028, ABP Biosciences) for showing dead cells (red fluorescence). The cells were then injected into a microchamber and subjected to acoustic waves generated by the middle subarray's two IDTs excited by an input signal with a voltage of 10 Vpp for 120 seconds. The whole acoustic exposure process is recorded in the supplementary movie S11. Recorded fluorescence images for a test group are given in Fig. R2.4 (a-d). We repeated the viability test procedure multiple times (N=21), as the used cell chamber only held a small number of cells. Fig. R2.4(e) summarizes the experimentally obtained cell viability data for N=152 cells, indicating a high cell viability of 99.3% after 120 seconds of acoustic exposure.

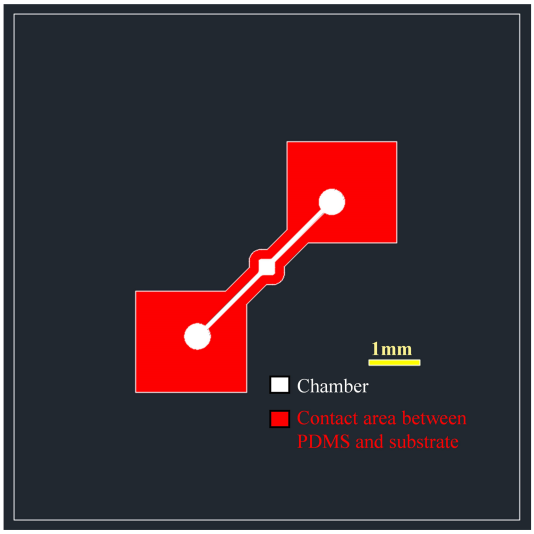

Fig. R2.1 Design of the microfluidic chamber of the JSAT device. Only the red region has PDMS in contact with the $LiNbO_3$ substrate.

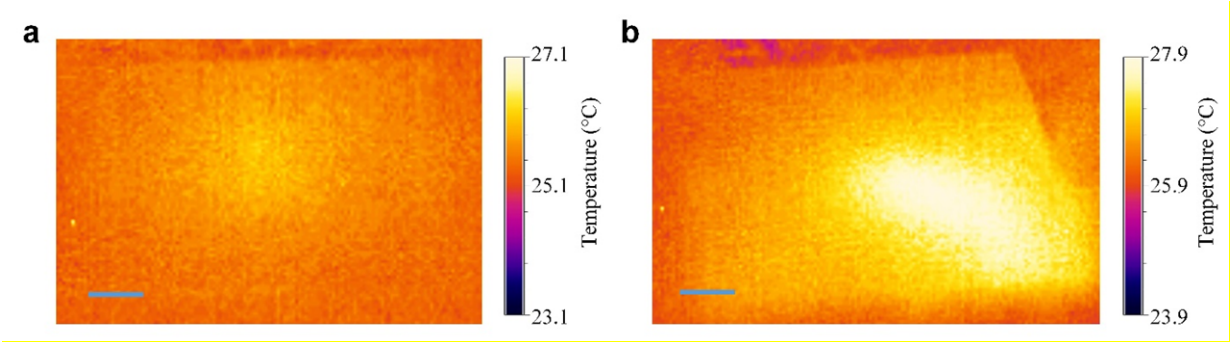

Fig. R2.2 Measured temperature on the back side of the substrate after 120 seconds. **(a)** Result for a pair of IDTs in the middle subarray excited with a 10 Vpp input. **(b)** Result for an IDT in the inner subarray excited with a 10 Vpp input. Scale bar: 5mm.

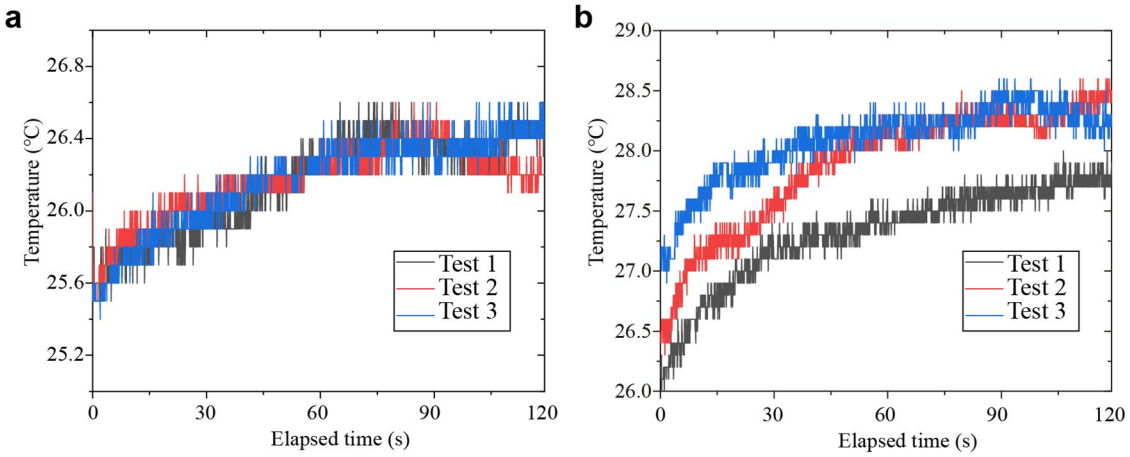

Fig. R2.3 Measured temperature from the back side of the substrate over time. **(a)** Result for a pair of IDTs in the middle subarray excited with a 10 Vpp input. **(b)** Result for an IDT in the inner subarray

excited with a 10 Vpp input.

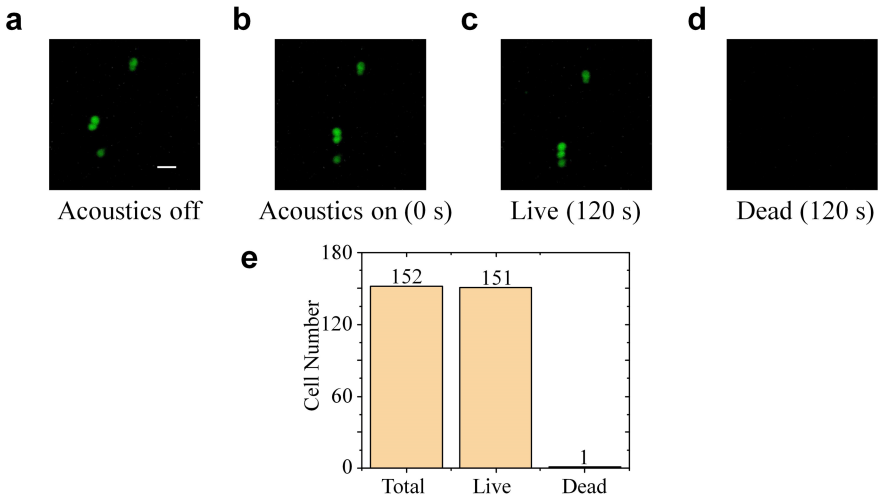

Fig. R2.4 **(a-c)** Images of the green fluorescence channel for three scenarios: **(a)** no acoustic waves applied, **(b)** acoustic waves turned on, **(c)** 120 seconds of acoustic exposure. In these images, the green dots are cells stained with calcium-AM. **(d)** Image of the red fluorescence channel acquired after 120 seconds of acoustic exposure (Scale bar: 40 μm). This image is black indicating no dead cells in that test group, due to the lack of uptake of propidium iodide. **(e)** Summarized cell viability data for all the N=152 cells in multiple tests (N=21).

Changes to the manuscript: Per the reviewer's comment, we made the following changes.

- In the Supplementary Information, we have added a new subsection: Supplementary Note 3. Characterization of device temperature and cell viability.
- In the "Cell deformation measurement", we updated the text: "In addition, we measured the SAW device's temperature, as well as the post-treatment cell viability. Their detailed procedures and results are in Supplementary Note 3 and Supplementary Figures 13-15."
- Four new supplementary figures are added:

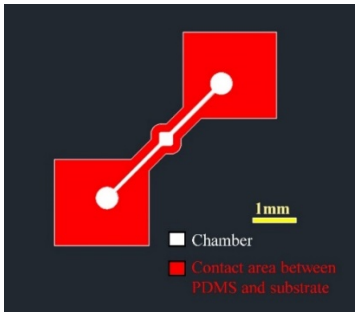

Supplementary Figure 12. Design of the microfluidic chamber of the JSAT device. Only the red region has PDMS in contact with the $LiNbO_3$ substrate.

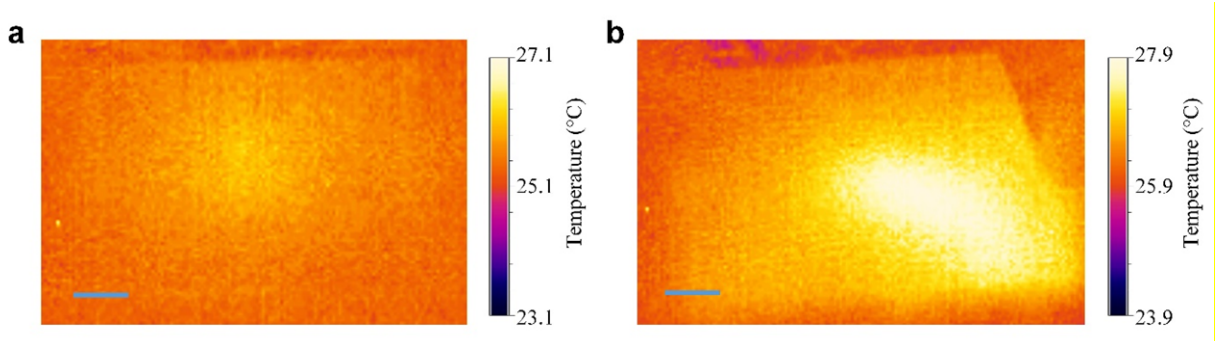

Supplementary Figure 13. Temperature fields measured from the back side of a substrate after 120 seconds. **(a)** Result for the case with a pair of IDTs in the middle subarray excited with a 10 Vpp input. **(b)** Result for the case with an IDT in the inner subarray excited with a 10 Vpp input. Scale bar: 5 mm.

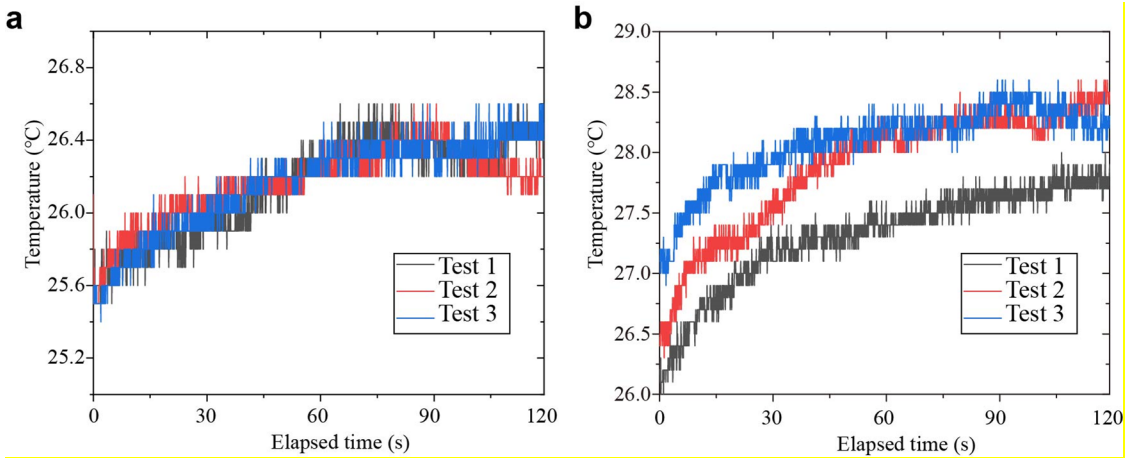

Supplementary Figure 14. Temperature change over time measured from the back side of the substrate. (a) Result for the case with a pair of IDTs in the middle subarray excited with a 10 Vpp input. **(b)** Result for the case with an IDT in the inner subarray excited with a 10 Vpp input.

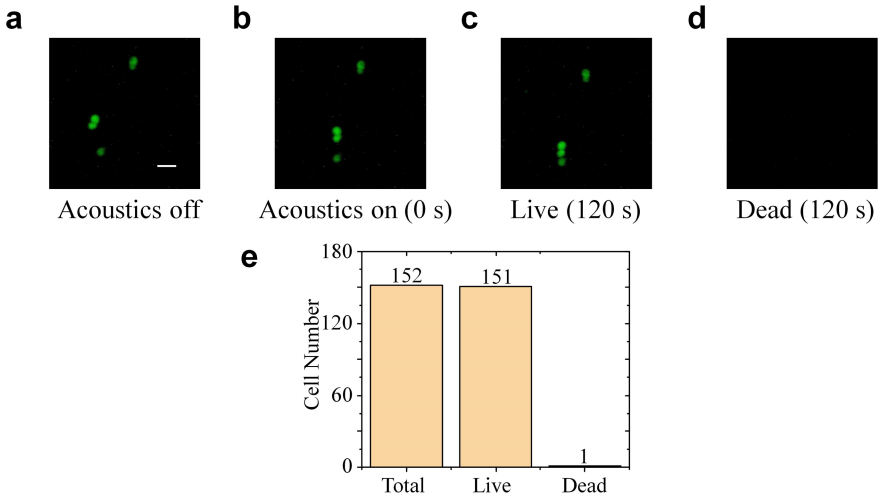

Supplementary Figure 15. Cell viability test results. (a-c) Images of the green fluorescence channel for three scenarios: **(a)** no acoustic waves applied, **(b)** acoustic waves turned on, **(c)** 120 seconds of acoustic exposure. In these images, the green dots are cells stained with Calcium-AM. **(d)** Image of the red fluorescence channel acquired after 120 seconds of acoustic exposure (Scale bar: 40 μm). This image is black indicating no dead cells in that test group, due to the lack of uptake of propidium iodide. **(e)** Summarized cell viability data for all the N=152 cells in multiple tests (N=21).

Comment 3: *From a physical point of view,*

(i) The model used to simulate acoustic streaming only accounts for Eckart bulk streaming, not boundary Rayleigh streaming. This should be both specified and justified in the manuscript. Indeed, according to the work by Bruus [Bruus H. 3D modeling of acoustofluidics in a liquid-filled cavity including streaming, viscous boundary layers, surrounding solids, and a piezoelectric transducer. Mathematics, (2019)], we could expect both bulk and boundary streaming to be significant in this type of configurations.

(ii) I do not understand why for the control of the z position (Fig 2d), the direction of the radiation force and streaming force are opposite to what was calculated in Ref. 2 (Fig. 4), while the devices look pretty similar. Could you please clarify this point?

Our response: We appreciate the reviewer's comment. Our responses to your comments (i) and (ii) are given below.

Response to (i): According to the work by Bruus (*Bruus H. 3D modeling of acoustofluidics in a liquid-filled cavity including streaming, viscous boundary layers, surrounding solids, and a piezoelectric transducer. mathematics, (2019).*), we have conducted three different streaming simulations with the

same acoustic pressure: (1) only boundary Rayleigh streaming; (2) only Eckart bulk streaming; and (3) acoustic streaming involving a combination of Rayleigh streaming and Eckart bulk streaming. These simulation results are given in Fig. R3.1a, R3.1b, and R3.1c, respectively. The maximum velocity of Rayleigh streaming in Fig. R3.1a is 3.5 μm/s, which is negligible compared to the velocity of Eckart bulk streaming, exceeding 100 μm/s, as shown in Fig. R3.1b. This observation is further corroborated by the velocity distribution comparison between Fig. R3.1b and Fig. R3.1c, which exhibits a similar pattern. This result is consistent with the work of Bach and Bruus (*Bach JS, Bruus H. Bulk-driven acoustic streaming at resonance in closed microcavities. Phys Rev E 100, 023104 (2019)*), where they simulated a horizontal 2×2, 4×4, and 6×6 streaming-roll pattern in a shallow square cavity. They found that the high-frequency 6×6 (2.24 MHz) streaming-roll pattern is dominated by the Eckart bulk streaming as opposed to the low-frequency 2×2 (0.75 MHz) streaming pattern, which is dominated by the boundary-driven streaming. In our acoustic device, the excitation frequencies for generating streaming patterns for cell rotations θ_x and θ_y are approximately 40 MHz, which is significantly higher than 2.24 MHz utilized in the Bruus setup. Per the reviewer's suggestion, we updated the simulation results by considering both bulk and boundary streaming.

Response to (ii): The early work (ref 2) contains an error in presenting the streaming direction. The drag force at the pressure node region should be in the downward direction, as presented in the studies of the Huang group (*Nama N, Barnkob R, Mao Z, Kähler CJ, Costanzo F, Huang TJ. Numerical study of acoustophoretic motion of particles in a PDMS microchannel driven by surface acoustic waves. Lab Chip 15, 2700-2709, 2015*) and other researchers (*Ni Z, et al. Modelling of SAW-PDMS acoustofluidics: physical fields and particle motions influenced by different descriptions of the PDMS domain. Lab Chip 19, 2728-2740, 2019*). Our study shows a downward drag force agreeing with previous studies.

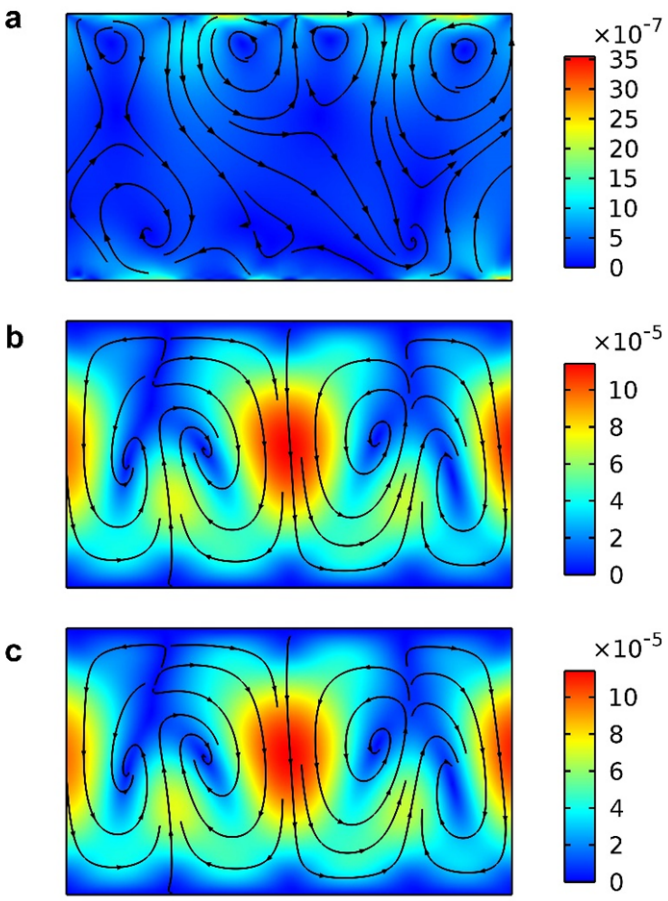

Fig. R3.1 Simulation results of acoustic streaming. **(a)** Boundary Rayleigh streaming. **(b)** Eckart bulk streaming. **(c)** Acoustic streaming field induced by the combination of Rayleigh streaming and Eckart bulk streaming.

Changes to the manuscript: Per the reviewer's comment, we made the following changes.

- In the "Supplementary Note 2. Numerical Simulation of acoustic streaming", we added the text: The top, bottom, left, and right boundaries of the fluid domain were set to the boundary velocity condition ($\mathbf{v}_{str}= \mathbf{v}^{bc}$)[5, 6], where $\mathbf{v}^{bc}$ is the slip velocity and can be calculated by[6]:

$$\mathbf{n}\cdot\mathbf{v}^{bc}=0, \qquad \text{(S7a)}$$

$$(1-\mathbf{nn})\cdot\mathbf{v}^{bc}=-\frac{1}{8\omega}\nabla_{\parallel}\left|\mathbf{v}_{1\parallel}\right|^{2}-\mathrm{Re}\left[\left(\frac{2-i}{4\omega}\nabla_{\parallel}\cdot\mathbf{v}_{1\parallel}^{*}+\frac{i}{2\omega}\partial_{\perp}\mathbf{v}_{1\perp}^{*}\right)\mathbf{v}_{1\parallel}\right], \qquad \text{(S7b)}$$

  where $\mathbf{v}_1$ is acoustic velocity in the bulk.
- Updated all simulation figures, including Fig.2d, Fig. S5a, Fig. S6a, Fig. S6d, Fig. S8a, Fig. S8d, Fig. S9a, Fig. S9b, Fig. S9c, Fig. S10a and Fig. S11a.

Comment 4: *In addition, time scales must be specified in all the figures and additional videos.*

Our response: We thank the reviewer for this comment. Per the reviewer's comment, time scales have been added to all the time-sequenced images and videos.

Reviewer: #3

Comment: *Novelty:*

This paper demonstrates the feasibility of combining in the same device, several operations related to translation, rotation, and deformation of a single cell by surface acoustic waves. A major novelty lies in that operations of translation, rotation, and deformation, which have been demonstrated separately before, are here combined in the same chip. It is impressive.

Our response: We extend our gratitude to the reviewer for their positive feedback on our work and for providing several insightful comments that have greatly contributed to the enhancement of the manuscript. We have thoroughly addressed all of the points raised in your review. Below, we provide detailed point-by-point responses to your comments.

Comment 1: *Major things:*

I realize that the authors have a challenge in explaining all the features of the device since it has so many degrees of freedom, and a journal paper is just in 2D. By just reading the manuscript it is difficult to understand if the method is robust and predictable. The videos helps. Nevertheless, I have some questions and comments. Overarching, it is difficult to understand to what extent the translations are predictable and if any calibrations are done.

Our response: We thank the reviewer for this comment. Elucidating all features of the device is indeed challenging. Therefore, to facilitate the explanation of the device design and mechanism, we labeled all the IDTs of the device and provided clear descriptions of the corresponding IDTs utilized for each manipulation task. This aims to assist readers in associating each described manipulation function with the activated IDTs, as depicted in Fig. 1. Additionally, experimental videos provide substantial validation of each manipulation function.

As the translational manipulation leverages the well-known phase modulation mechanism, *i.e.*, changing the phase difference between input signals for a pair of standing wave transducers, the translation process is highly predictable. Moreover, this phase adjustment-based translation mechanism has been successfully demonstrated in many previous studies (Guo F, *et al.* Three-dimensional manipulation of single cells using surface acoustic waves. *Proc Natl Acad Sci* **113**, 1522-1527, 2016; Drinkwater BW. Dynamic-field devices for the ultrasonic manipulation of microparticles. *Lab on a Chip* 16, 2360-2375, 2016; Courtney CRP, *et al*. Manipulation of particles in two dimensions using phase controllable ultrasonic standing waves. *Proceedings of the Royal Society a-Mathematical Physical and Engineering Sciences*, 468, 337-360, 2012). Hence, for the experiments in this study, we didn't perform calibration for the translational manipulation.

Changes to the manuscript: Per the reviewer's comments, in subsection "3D translation via JSAT", we added the following text: "As shown in Fig. S3, the actual cell positions closely agree with the predicted positions using relations $u_x=\Delta\varphi_x\lambda^{out}/(4\pi)$ and $u_y=\Delta\varphi_y\lambda^{out}/(4\pi)$. As the phase modulation-based translational manipulation mechanism is known for its good predictability[2], we didn't perform any calibration before translating an MCF7 cell following complex trajectories."

Comment 2: *What parameters are controlled in the Matlab code? Which of these are kept constant during the operation and which are being adjusted? Please describe the main features of the program.*

Our response: We thank the reviewer for this comment. For the used Tektronix function generators, we can use Matlab codes to control each channel's output phase, frequency, and amplitude. To translate a cell trapped in a potential well, the input frequencies and voltages were not changed, while the input phases were changed. The key features of our customized program include adjusting the phases, frequencies, and amplitudes of multiple signal channels, as well as gradually changing the phases following predetermined sequences of phases for achieving step-by-step translation of a cell.

Changes to the manuscript: Per the reviewer's comments, in the subsection "Device operation", we have added the following text: "To translate a cell along the desired complex paths, the frequencies and voltages for the IDTs remain constant, while shifts are made to the input phases. The phase shifts are automatically performed using customized MATLAB codes, having key features including adjusting the phases, frequencies, and amplitudes of multiple signal channels, as well as gradually changing the phases following predetermined sequences of phases for achieving step-by-step translation of a cell."

Comment 3: *Please describe how the motion of a cell is programmed, like when you make the letters 'D', 'U', 'K', 'E'. Can you program an arbitrary trajectory based on a rule or a function, or it must be tweaked? Do you need to calibrate the phase shift necessary to achieve a certain translation? It would be very convincing if you could overlay the intended trajectory with the measured trajectory.*

Our response: We thank the reviewer for this comment. The letters 'D', 'U', 'K', 'E', and any arbitrary trajectory can be segmented into a sequence of steps, where the components in the x- and y-directions of each step are constrained to be smaller than one quarter of a wavelength. Otherwise, the cell will relocate to the nearest pressure node rather than the intended destination. For each step, denoted by a displacement vector $\mathbf{u} = [u_x, u_y, 0]$, translation in the x- or y-direction can be achieved by adjusting the phase difference between the interdigital transducers (IDTs) in the corresponding direction. When the phase differences change from $\boldsymbol{\varphi}$ to $\boldsymbol{\varphi}+\Delta\boldsymbol{\varphi}$, where $\boldsymbol{\varphi} = [\varphi_x, \varphi_y]$ and $\Delta\boldsymbol{\varphi} = [\Delta\varphi_x, \Delta\varphi_y]$, the desired short

translation **u** = [u_x, u_y, 0] of the trapped cell can be realized with predictable displacement components $u_x=\Delta\varphi_x\lambda^{out}/(4\pi)$ and $u_y=\Delta\varphi_y\lambda^{out}/(4\pi)$. Utilizing this approach, the desired sequence of phase differences can be determined for a desired arbitrary-shaped trajectory. This phase sequence can be gradually applied by using MATLAB codes that control all the channels of the used function generators.

For our translation experiment, we didn't perform any calibration, as the phase modulation-based translation mechanism is known for its good predictability (Guo F, *et al.* Three-dimensional manipulation of single cells using surface acoustic waves. *Proc Natl Acad Sci* **113**, 1522-1527, 2016; Drinkwater BW. Dynamic-field devices for the ultrasonic manipulation of microparticles. *Lab on a Chip* 16, 2360-2375, 2016; Courtney CRP, *et al*. Manipulation of particles in two dimensions using phase-controllable ultrasonic standing waves. *Proceedings of the Royal Society a-Mathematical Physical and Engineering Sciences*, 468, 337-360, 2012). In Fig. R1, the acquired cell images are overlayed with predicted positions (orange dots in Fig. R1), showing that the actual cell positions agree with the predicted locations.

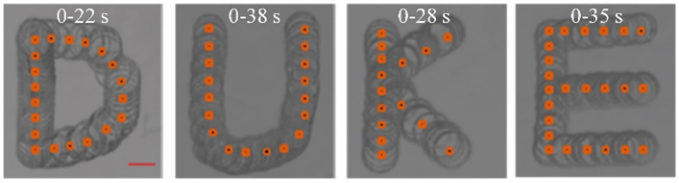

Fig. R1: Stacked microscopic images extracted from recorded videos during cell translation processes. The orange points mark positions predicted by the phase modulation-based translation method.

Changes to the manuscript: Per the reviewer's comment, we made the following changes.

- In the "3D translation *via* JSAT" section, we added the text: "As shown in Fig. S3, the actual cell positions closely agree with the predicted positions using relations $u_x=\Delta\varphi_x\lambda^{out}/(4\pi)$ and $u_y=\Delta\varphi_y\lambda^{out}/(4\pi)$. As the phase modulation-based translational manipulation mechanism is known for its good predictability[2], we didn't perform any calibration before translating an MCF7 cell following complex trajectories."
- Added Supplementary Figure 3:

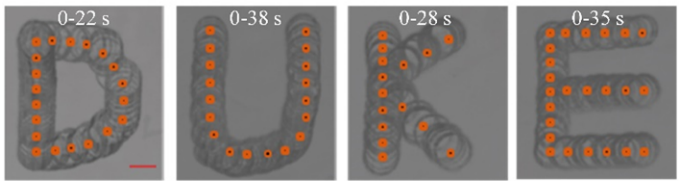

Supplementary Figure 3. Comparisons between actual and predicted cell positions for four cases of translating a cell to depict 'D,' 'U,' 'K,' and 'E'. For each case, images are extracted from a recoded video and then stacked. Each stacked image is overlayed with orange dots, representing positions predicted

by the phase modulation-based translation approach. Scale bar: 10 μm.

Comment 4: *Looking at movies S3 and S4, I do not understand how a symmetric streaming field can lead to rotation of the cell if it is positioned in the center of the channel. I would expect the net rotation to be zero. I understand that when a cell is held in position by one acoustic field while the fluid is streaming vigorously, it is likely that it will gain some net rotation, but how can it be predicted? Again, is it programmed from first principles, or does one need to find suitable combinations of sound fields by scanning through frequencies, amplitudes, and phase shifts?*

Our response: We thank the reviewer for this comment. Actually, the two streaming vortices adjacent to the trapped cell are not perfectly symmetrical. When input amplitudes for two IDTs are different, for two streaming vortices at different sides of a pressure node, the streaming velocity in one vortex is slightly higher than in the other. To better elucidate this mechanism, we performed numerical simulations with the excitation voltage V_2^{mid} for IDT_2^{mid} slightly higher than the voltage V_4^{mid} for IDT_4^{mid}. As shown in Fig. S6, the streaming fields of vortices on different sides of a pressure node become slightly asymmetric. These asymmetric vortices can lead to a non-zero viscous torque applied on the cell, consequently inducing cell rotation. As revealed by our simulation results in Fig. S5d and S5e, the asymmetric vortices lead to cell rotation in the $+\theta_x$-direction. The experimental results exhibit a good consistency with the numerical predictions.

Changes to the manuscript: Per the reviewer's comment, in the "3D rotation via JSAT" section, we have updated the writing using the following text: "Moreover, our simulation results (Fig. S6d and S6e) reveal that the tangential streaming velocities can lead to cell rotation in the $+\theta_x$-direction being dominant. Furthermore, during the streaming-induced cell rotation, the acoustic potential well generated by the standing SAWs can still effectively trap the cell, ensuring no translational motion or eccentricity. The experimental validation results (top of Fig. 3b and movie S3) show that an MCF7 cell could be successfully trapped and rotated in the $+\theta_x$-direction when $V_4^{mid} < V_2^{mid}$, agreeing with the numerically predicted rotation direction. Therefore, we can reliably execute the rotational manipulation as planned."

Comment 5: *If I understand it correctly, the rotation around x- and y is governed by the 'mid' transducers. How can a cell rotate consistently while moving across a streaming field that is not constant? Or do you need to adjust the 'mid' transducer for each position? Describe how this is done.*

Our response: We thank the reviewer for this comment. The combined (translation + rotation) motions can be divided into two categories: (1) the translation axis and the rotation axis are the same and (2)

the translation axis and the rotation axis are orthogonal. The manipulation mechanisms for these two categories are explained below.

Category 1 (the translation axis and the rotation axis are the same): For example, to achieve combined translation u_x and rotation θ_x, we can change the input phase difference for IDT_1^{out} and IDT_3^{out} of the outer subarray to control the translation u_x, as well as change input amplitudes for IDT_2^{mid} and IDT_4^{mid} to generate streaming for controlling rotation θ_x. As illustrated in Figure 4a, the two streaming vortex tunnels are parallel to the cell translation direction, and the cell translates along a line between the two streaming tunnels. Because of this mechanism, our device can achieve combined translation u_x and rotation θ_x.

Category 2 (the translation axis and the rotation axis are orthogonal): For example, to achieve combined translation u_x and rotation θ_y, we can change the input phase difference for IDT_1^{mid} and IDT_3^{mid} of the mid subarray to control the translation u_x, as well as change input amplitudes for IDT_1^{mid} and IDT_3^{mid} to generate streaming for controlling rotation θ_y. When translating a cell through phase modulation, the positions of two streaming vortex tunnels (see Figure 4c) shift synchronously, thus ensuring continuous cell rotation during the translation process.

Changes to the manuscript: Per the reviewer's comments, we have included a detailed illustration in Section "Simultaneous translation and rotation *via* JSAT".

- As the *x*-axis standing SAW generated from $\{IDT_1^{out}, IDT_3^{out}\}$ exhibits negligible impact on the streaming vortices generated by $\{IDT_2^{mid}, IDT_4^{mid}\}$ and the two streaming vortex tunnels are parallel to the cell translation direction, our approach achieves continuous cell rotation during the translation process.
- Moreover, when translating a cell through phase modulation, the positions of two streaming vortex tunnels (illustrated in Fig. 4c) shift synchronously, thus ensuring continuous cell rotation during the translation process.

Comment 6: *The z-translation has quite limited data. What is the range that you can translate the cell? How fast does it respond to a change in amplitude? I.e. does it rely on sedimentation to go down or the streaming takes care of it?*

Our response: We thank the reviewer for this comment. The translational range of a cell along the z-axis is constrained by the height of the microfluidic chamber, which is 60 μm in our JSAT device. The maximum z-translation range also needs to consider the cell diameter. For example, for a cell with a diameter of D=10 μm loaded in a chamber with a height of H=60 μm, its z-translation range is limited

to approximately H-D=50 μm. As illustrated in Fig 2d (right), the gravity and streaming-induced drag force are downward, whereas the acoustic radiation force is upward (*i.e.*, in the +z-direction) acting as the z-motion driving force. The +z-directional cell translation is enabled by turning on acoustic waves. Once acoustic waves are off, the cell sinks very slowly, as the densities of most cells are slightly greater than the culture medium's density.

Changes to the manuscript: Per the reviewer's comment, we made the following changes.
In the "3D translation *via* JSAT", we updated and added the text: "which points to the +z-direction acting as the levitation driving force" and "The out-of-plane translation u_z depends on the interplay of all the out-of-plane forces, including the position-dependent acoustic radiation and drag forces, the buoyancy force F_{Buo}, and the gravitational force F_g, as shown in Fig. 2d (right). Most cells, including MCF7 cells, have a density slightly higher than the culture medium (water with additives) and the inertia of a microscale cell could be ignored, enabling z-directional manipulation by applying acoustic waves and stopping inputting power at the desired position. The cell remains at the position for a while since it sinking very slowly. Therefore, the control of out-of-plane translation cannot be as precise and stable as the control of in-plane translation due to the absence of a Gor'kov potential well-like trap. Additionally, when the cell experiences other motions, especially rotations, they affect the out-of-plane translation. The out-of-plane translation precision is also affected by the two-dimensional imaging nature of our current microscope, as the translation is difficult to be quantitively characterized."

Comment 7: *Cell deformation has previously been demonstrated experimentally and theorized upon in the realm of bulk-acoustic waves, some works of which should be cited IMHO (DOI: 10.1103/physreve.99.063002, DOI: 10.1063/5.0122017, DOI: 10.1039/c9lc00999j, DOI: 10.1063/1.4882777).*

Our response: We thank the reviewer for this comment and bringing these critical papers to our sight. Our approach differs from those studies, as it uses SAWs and a different mechanism to deform cells (*i.e.*, SAW streaming induced cell rotation and shear). The revised manuscript has cited those important studies based on bulk acoustic waves.

Changes to the manuscript: Per the reviewer's comments, previous studies on bulk acoustic waves-based cell deformation have been cited. Moreover, in the "Introduction" section, we have added the following text: "In addition to translational and rotational object manipulation, bulk acoustic wave- and streaming-based approaches have been developed to deform cells[63-66]."

63. Mishra P, Hill M, Glynne-Jones P. Deformation of red blood cells using acoustic radiation forces. Biomicrofluidics

8, (2014).
64. Link A, Franke T. Acoustic erythrocytometer for mechanically probing cell viscoelasticity. Lab Chip 20, 1991-1998 (2020).
65. Silva GT, et al. Acoustic deformation for the extraction of mechanical properties of lipid vesicle populations. Phys Rev E 99, 063002 (2019).
66. Liu Y, Xin F. Deformation dynamics of spherical red blood cells in viscous fluid driven by ultrasound. Phys Fluids 35, (2023).

Comment 8: *Minor things:*

The start of movie S3 is a bit chaotic and it is not easy to observe the streaming field at the beginning.

Our response: We thank the reviewer for this comment. At the beginning of movie S3, we present the particle motion in the absence of acoustics, resulting in particles exhibiting chaotic behavior. In accordance with the reviewer's comment, we have labeled this state at the start of movie S3.

Change to the manuscript: We have updated movie S3 to include a label indicating the state with acoustic waves off.

Comment 9: *Fig 2D, streaming arrows are too small.*

Our response: We thank the reviewer for this comment. We have updated Fig 2D.

Change to the manuscript: Per the reviewer's comments, we have enlarged the streaming arrows in Fig. 2D.

Comment 10: *Figure S1 and S2: Show scale bar.*

Our response: We thank the reviewer for this comment. Per the reviewer's comments, scale bars have been added to both figures.

Changes to the manuscript: Per the reviewer's comment, we updated the two figures to include scale bars.

REVIEWERS' COMMENTS

Reviewer #1 (Remarks to the Author):

The authors have clearly and comprehensively addressed the issues I raised in the review. I was very pleased to see the very positive results on cell viability, which I think adds to the impact of the work considerably. Hence I am happy to see this work published in its revised form.

Reviewer #2 (Remarks to the Author):

The authors have carefully addressed my remarks. I now fully recommend publication of the paper.

Reviewer #3 (Remarks to the Author):

The authors have responded to my previous comments and made appropriate changes to the manuscript.

I have one additional comment spurred by the included viability testing. I appreciate the effort made to investigate temperature and viability. However, it is my impression from the procedure you describe that the cells were first stained with live and dead stain and then exposed to sound in the device while recording the fluorescence for the two dyes. In my understanding such a protocol reports the state of the cell at the time of staining and is normally not used for continuous monitoring. If a cell would be damaged during the exposure, how could they attain a signal from propidium iodide (PI) unless there is free PI molecules present in the medium during the exposure? Second, if you expect that the live stain would leak out in the case of damage, then please clarify this in the manuscript and include a reference regarding continuous monitoring of live staining. Please clarify in the manuscript the limitations of the viability test. To me it seems that you can possibly conclude that there is no apparent damage to the cells (since no live stain leaks out) but that long-term effects have not been investigated, e.g. ability to proliferate, DNA damage, function, etc. You could also argue in the manuscript that there is very little evidence in the

literature that acoustic manipulation causes cell damage (Wiklund has written about this for instance).

Per Augustsson
Lund University

Itemized list of response to reviewers' remarks

(*Black italic: Editor's remarks*; Blue type: Our response; Additions/modifications to the manuscript and Supplementary Materials are highlighted in yellow)

Reviewer: #3

Comment: *The authors have responded to my previous comments and made appropriate changes to the manuscript.*

I have one additional comment spurred by the included viability testing. I appreciate the effort made to investigate temperature and viability. However, it is my impression from the procedure you describe that the cells were first stained with live and dead stain and then exposed to sound in the device while recording the fluorescence for the two dyes. In my understanding such a protocol reports the state of the cell at the time of staining and is normally not used for continuous monitoring. If a cell would be damaged during the exposure, how could they attain a signal from propidium iodide (PI) unless there is free PI molecules present in the medium during the exposure? Second, if you expect that the live stain would leak out in the case of damage, then please clarify this in the manuscript and include a reference regarding continuous monitoring of live staining. Please clarify in the manuscript the limitations of the viability test. To me it seems that you can possibly conclude that there is no apparent damage to the cells (since no live stain leaks out) but that long-term effects have not been investigated, e.g. ability to proliferate, DNA damage, function, etc. You could also argue in the manuscript that there is very little evidence in the literature that acoustic manipulation causes cell damage (Wiklund has written about this for instance).

Our response: We appreciate the reviewer's insightful comments regarding the cell viability testing. In our experiment, cells were initially stained with calcium AM for live cells and propidium iodide (PI) for dead cells before being exposed to acoustic waves. We acknowledge that our viability test has limitations, as cells that die post-staining may not show the fluorescence of PI due to the absence of PI dye in our device. We agree that the viability protocol used in this study is limited to demonstrating no apparent damage to the cells but is not capable of revealing long-term effects on proliferation rate, DNA damage, or cell function.

Changes to the manuscript: Per the reviewer's comment, we made the following changes.

- Updated the caption for Supplementary Figure 15 (d) using the following text: "Image of the red fluorescence channel. This image is black indicating no dead cells before applying acoustic waves. Before loading cells into our device, they were stained with calcium AM for revealing

live cells and propidium iodide (PI) for dead cells."

- In the "Supplementary Note 3. Characterization of device temperature and cell viability" section, we added the following text: "Note that this viability result is obtained by calculating the ratio of cells with green fluorescence to the total number of cells. The red fluorescence emitted by PI only reveals cells that were dead before exposure to acoustic waves, as the PI staining was performed before loading the cells into our acoustic device. This PI stain could not detect cells that died as a result of acoustic exposure due to the absence of PI dye in the cell manipulation device. For a cell stained with calcium-AM, its transition from live to dead can be revealed through the loss of its fluorescence intensity, as the marker leaks out of the cell, a consequence of increased membrane permeability[10]. In our captured microscopic images taken at different times, nearly all cells showed no significant change in fluorescence when exposed to acoustic waves. This suggests that our acoustic tweezers do not cause significant cell damage. Numerous other studies have demonstrated that their acoustic tweezers do not result in significant cellular damage[8, 11, 12]. To gain further insights into the long-term effects of our acoustic tweezers, aspects such as the proliferation rate, DNA damage, and cell functionality still need to be characterized."

10. Radošković K, de Grooth BG, Greve J. Changes in intracellular calcium concentration and pH of target cells during the cytotoxic process: A quantitative study at the single cell level. Cytometry 20, 281-289 (1995).

11. Olofsson K, et al. Acoustic formation of multicellular tumor spheroids enabling on-chip functional and structural imaging. Lab Chip 18, 2466-2476 (2018).

12. Baudoin M, et al. Spatially selective manipulation of cells with single-beam acoustical tweezers. Nat Commun 11, 4244 (2020).